Journal of Experimental Botany, Vol. 71, No. 7 pp. 2351–2361, 2020
doi:10.1093/jxb/erz494 Advance Access Publication 3 November, 2019
This paper is available online free of all access charges (see https://academic.oup.com/jxb/pages/openaccess for further details)

RESEARCH PAPER

Storing carbon in leaf lipid sinks enhances perennial ryegrass carbon capture especially under high N and elevated CO_2

Zac Beechey-Gradwell[1,2,*], Luke Cooney[1], Somrutai Winichayakul[1], Mitchell Andrews[2], Shen Y. Hea[1], Tracey Crowther[1] and Nick Roberts[1]

[1] Agresearch Grasslands, Tennent Drive, Fitzherbert, Palmerston North 4410, New Zealand
[2] Faculty of Life Sciences, Lincoln University, Lincoln 7647, New Zealand

* Correspondence: Zac.Beechey-Gradwell@agresearch.co.nz

Received 3 September 2019; Editorial decision 28 October 2019; Accepted 29 October 2019

Editor: Tracy Lawson, University of Essex, UK

Abstract

By modifying two genes involved in lipid biosynthesis and storage [cysteine oleosin (cys-OLE)/diacylglycerol *O*-acyltransferase (DGAT)], the accumulation of stable lipid droplets in perennial ryegrass (*Lolium perenne*) leaves was achieved. Growth, biomass allocation, leaf structure, gas exchange parameters, fatty acids, and water-soluble carbohydrates were quantified for a high-expressing cys-OLE/DGAT ryegrass transformant (HL) and a wild-type (WT) control grown under controlled conditions with 1–10 mM nitrogen (N) supply at ambient and elevated atmospheric CO_2. A dramatic shift in leaf carbon (C) storage occurred in HL leaves, away from readily mobilizable carbohydrates and towards stable lipid droplets. HL exhibited an increased growth rate, mainly in non-photosynthetic organs, leading to a decreased leaf mass fraction. HL leaves, however, displayed an increased specific leaf area and photosynthetic rate per unit leaf area, delivering greater overall C capture and leaf growth at high N supply. HL also exhibited a greater photosynthesis response to elevated atmospheric CO_2. We speculate that by behaving as uniquely stable microsinks for C, cys-OLE-encapsulated lipid droplets can reduce feedback inhibition of photosynthesis and drive greater C capture. Manipulation of many genes and gene combinations has been used to increase non-seed lipid content. However, the cys-OLE/DGAT technology remains the only reported case that increases plant biomass. We contrast cys-OLE/DGAT with other lipid accumulation strategies and discuss the implications of introducing lipid sinks into non-seed organs for plant energy homeostasis and growth.

Keywords: Carbon dioxide, lipid, *Lolium perenne*, metabolic engineering, nitrogen, photosynthesis, source–sink, triacylglycerol.

Introduction

Greater yields from major crops are required to ensure food security in the face of growing global demand for food and energy. Two compelling strategies for enhancing food security are increasing photosynthesis (Long *et al.*, 2006) and engineering higher levels of valuable nutrients such as lipids into plant tissues (Vanhercke *et al.*, 2019). Genetic manipulation of CO_2 capture and light energy use efficiency could feasibly enhance photosynthesis, growth, and yield (Wu *et al.*, 2019). However, translating improved photosynthesis into greater yields will depend upon the capacity of plants to effectively utilize or store additional photosynthates through sink development (Paul and Foyer, 2001; White *et al.*, 2016).

Plant-derived oils are an economically valuable, energy-dense carbon (C) sink in plants; containing ~38 kJ g^{-1}. Present

annual (2017/2018) global production of plant oils is 204 Mt, the clear majority of which is seed derived. Since non-seed vegetative organs such as leaves make up a large proportion of crop biomass, metabolic engineering of higher triacylglycerol (TAG) levels into these organs is viewed as an attractive prospect for boosting per hectare oil yields (Napier *et al.*, 2014). A number of groups have now reported large and sustained increases in TAG in leaves and other non-seed organs, some of which are being tested in the field as oil production platforms (Hofvander *et al.*, 2016; Zale *et al.*, 2016). However, many studies also report plant growth penalties associated with oil accumulation (see Vanhercke *et al.*, 2019, and references therein).

Long-term storage of lipids in the leaves and roots of Arabidopsis (*Arabidopsis thaliana*), mainly in the form of TAG, was achieved when the diacylglycerol *O*-acyltransferase (DGAT, EC 2.3.1.20) enzyme was co-expressed with cysteine oleosin (cys-OLE). This novel lipid droplet-encapsulating protein slowed the degradation of lipid droplets in vegetative tissues, and *in vitro* in the presence of cysteine protease (Winichayakul *et al.*, 2013). Remarkably, an increase in photosynthesis and shoot biomass was also observed in cys-OLE/DGAT Arabidopsis, which was initially speculated to be the result of a CO_2-recycling phenomenon associated with higher *de novo* fatty acid (FA) synthesis (Schwender *et al.*, 2004; Winichayakul *et al.*, 2013).

Perennial ryegrass (*Lolium perenne*) is the most widely used plant species in pastoral agriculture in temperate regions, due to its balanced seasonal dry matter production and tolerance of defoliation (Chapman *et al.*, 2012). However, the productivity of animals grazing perennial ryegrass is constrained by the low energy density of the leaves (Kingston-Smith and Theodorou, 2000). Cys-OLE/DGAT expression in perennial ryegrass leaves could deliver the benefits of higher lipids in animal diets in a cost-effective manner. Given that storage of TAG in the roots of forage grasses is of little practical benefit, the cys-OLE/DGAT technology has been expressed under green tissue-specific promoter sequences in perennial ryegrass, delivering consistently high leaf lipids under repetitive defoliation (Beechey-Gradwell *et al.*, 2018).

It is now pertinent to ask how cys-OLE/DGAT expression in perennial ryegrass leaves will influence the physiology of C assimilation under diverse growing conditions. Plant-available nitrogen (N) is a major driver of crop growth and occurs in the soil primarily in two forms; nitrate (NO_3^-) and ammonium (NH_4^+), each of which has distinct effects on photosynthesis (Guo *et al.*, 2007) and plant growth (Andrews *et al.*, 2013). Elevated atmospheric CO_2 levels (e[CO_2]) can increase photosynthesis in the short term; however, if photosynthate utilization is inadequate, a source–sink imbalance can arise, leading to end-product (carbohydrate) accumulation and subsequent down-regulation of photosynthesis (Ainsworth *et al.*, 2004, 2007). It has also been disputed whether N form influences the way that plants respond to e[CO_2] (Bloom, 2015; Andrews *et al.*, 2019).

In this study, we describe a technology designed to allow stable leaf lipid droplets to accumulate in perennial ryegrass leaves (cys-OLE/DGAT). We screened cys-OLE/DGAT ryegrass lines with a range of leaf FA levels and selected a high expressing transformant for growth, biomass allocation, leaf structure, gas exchange, and water-soluble carbohydrate (WSC) analysis under 1–10 mM NO_3^- and NH_4^+ supply at ambient and elevated atmospheric CO_2. The response of photosynthetic parameters to e[CO_2] revealed effects of leaf cys-OLE/DGAT expression on perennial ryegrass sink–source coordination. We are the first to report, in detail, on the C assimilation physiology associated with the inherently faster growth of plants expressing cys-OLE/DGAT.

Materials and methods

Plant material and experimental layout

The untransformed WT control genotype 'IMPACT 566' used throughout this work was derived from the perennial ryegrass (*Lolium perenne*) cultivar 'Grasslands Impact' which was selected for its amenability to transformation and regeneration. Replicate plants in all experiments consisted of vegetative clonal ramets of WT or independent WT transformation events. Therefore, the transgenic genotypes differed genetically from the WT only in the presence of the cys-OLE/DGAT construct, while the transgenic genotypes differed genetically from one another only in the position and copy number of the cys-OLE/DGAT construct in the genome.

Experiments were conducted either in the glasshouse or in controlled-environment growth chambers. Total leaf FA and recombinant protein content were initially determined for the WT, a vector control (VC), and 12 independent transgenic cys-OLE/DGAT genotypes, grown in the glasshouse under regular mechanical defoliation. The WT, VC, and the transgenic genotypes '3501' and '3807' were also analysed for leaf TAG and root FA content, with samples taken ~3 weeks after defoliation (n=6–8). The WT and the transgenic genotypes '3501' and '6205' were used in a preliminary regrowth trial at ambient [CO_2] (a[CO_2]) and e[CO_2] across two growth chambers. Then, in the main experiment described in this study, the same growth chambers (with identical settings, described below) were used for a detailed physiological comparison of the WT and the high-expressing genotype '6205' (HL), in a formal regrowth trial at a[CO_2] and e[CO_2] under different levels of NO_3^- and NH_4^+ supply.

SDS–PAGE analysis of DGAT and Cys-OLE

Protein samples were prepared by collecting fresh or 10 mg DW of finely ground leaf in 150 µl of sterile H_2O, 200 µl of 2× protein loading buffer [1:2 diluted 4× lithium dodecyl sulfate sample buffer (Life Technologies), 8 M urea, 5% (v/v) β-mercaptoethanol, and 0.2 M DTT]. The mixtures were totally homogenized then heated at 70 °C for 10 min, centrifuged at 20 000 *g* for 30 s, and the soluble protein suspension was collected. Equal quantities of protein were separated by SDS–PAGE (Mini-PROTEAN® TGX stain-free™ pre-cast gels, Bio-Rad) and blotted onto a Bio-Rad polyvinylidene difluoride membrane for the DGAT immunoblot. Equal quantities of protein were separated on a gradient 4–12% Bis-Tris gel (NUPAGE; Life Technologies) and blotted onto nitrocellulose membrane for the cys-OLE immunoblot. Immunoblotting was performed as described in Winichayakul *et al.* (2013). Chemiluminescent activity was developed using Advansta WesternBright ECL spray and visualized by the Bio-Rad ChemiDoc™ imaging system.

Establishment phase

In the main experiment described in this study, WT and HL clones were made from mature plants by splitting them into ramets consisting of 3–4 tillers and cutting to 10 cm of combined root and shoot length. Approximately 200 clonal ramets of each genotype were generated and placed in individual cylindrical plastic pots containing washed sand (1.6 litres). The ramets were given 23 d to establish a root system in

a Conviron BDW 120 plant growth room at ambient CO_2 (Thermo-Fisher, Auckland, New Zealand). Metal halide bulbs (400 W Venture Ltd, Mount Maunganui, New Zealand) and soft tone, white incandescent bulbs (100 W, Philips, Auckland, New Zealand) provided ~500±50 µmol photosynthetically active radiation (PAR) m^{-2} s^{-1} as white light, under a 12 h photoperiod, with light levels ramping at dawn/dusk for 60 min. The day/night temperature and relative humidity (RH) were 20/15 °C and 60/68%, respectively. A top-down airflow pattern, with a controlled flow of outdoor air, maintained ambient atmospheric CO_2 levels (~400 ppm CO_2). During the establishment period, pots were flushed with 100 ml of basal nutrient medium described in Andrews *et al.* (1989) containing 2 mM KNO_3, three times per week. We found that supplying suboptimal NO_3^- limited establishment phase growth enough to avoid 'pot-limited' conditions (Poorter *et al.*, 2012) early in the subsequent regrowth phase, while also avoiding severe 'transplanting shock'. At the end of the establishment phase, plants were defoliated and the DW of leaf clippings from 5 cm above the pot media surface was determined after oven-drying at 80 °C overnight. Of the 200 clones of each genotype generated, 140 were selected for use in the experimental regrowth phase. Selection was based on the leaf DW at the end of the establishment phase, which averaged 0.118±0.036 g for the WT genotype and 0.113±0.020 g for the HL genotype (mean ±SD, n=140). A subset of defoliated plants (n=5) were destructively sampled at this time, oven dried, and weighed for 'sheath' (0–5 cm from the pot surface) and root DW, enabling the later calculation of relative growth rate (RGR).

Experimental regrowth phase

Following defoliation of the established plants, half of the material was moved into a second Conviron BDW 120 plant growth room, with identical settings to those described above, except that the CO_2 level was maintained at 760 ppm with G214 food grade CO_2 (BOC, Auckland, New Zealand). The two cabinets were previously tested for uniformity (Andrews *et al.*, 2019). The CO_2 levels in both growth rooms were measured continuously using PP Systems WMA-4 Gas Analysers (John Morris Scientific, Auckland, New Zealand). Pots were randomly allocated to different N treatments (n=5) then flushed with 150 ml of basal nutrient medium containing either 1, 2, 3, 4, 5, 7.5, or 10 mM N as either NO_3^- or NH_4^+ every 2 d for the regrowth phase. The pH of the nutrient media solutions was in the range of 5.4–5.6. Potassium concentrations were balanced in all cases with the highest potassium treatment (10 mM) using K_2SO_4, but sulfate was not balanced.

Gas exchange measurements

Between days 21 and 28 of the regrowth phase, plants treated with a high N supply (5–7.5 mM) were sampled for measurements of net photosynthesis under saturating irradiance (A_{sat}), specific leaf area (SLA), photosynthesis response to intracellular CO_2 (A/C_i), and the ratio of Rubisco oxygenation/carboxylation (V_o/V_c). A_{sat} and A/C_i analysis was carried out using a using a LiCor 6400XT (LiCor Biosciences, Lincoln, NE, USA) with a 6 cm^2 leaf chamber. The three youngest fully expanded leaves per replicate pot were given 15–20 min to adjust to the following chamber conditions: CO_2 was supplied at the growth room CO_2 level, light was supplied at 1500 µmol PAR m^{-2} s^{-1}, leaf temperature was 23 °C, flow rate was 300 µmol s^{-1}, and sample RH was maintained at 65–75%. After 15–20 min, net photosynthesis was logged. The CO_2 supply was then subsequently decreased stepwise to 50 ppm, then taken back up to 1300 ppm, with 2–3 min adjustment time per measurement. A/C_i data were modelled according to Sharkey *et al.* (2007) to give estimates of the maximum velocity of Rubisco carboxylation ($V_{c,max}$), the rate of electron transport, and mesophyll conductance to CO_2 (g_m). To improve the A/C_i model outputs, we substituted our accurate estimate of the CO_2 compensation point in the absence of dark respiration in the light (see Supplementary Table S1A at *JXB* online) into the model, as recommended by Sharkey (2016). After gas exchange analysis, the leaves were photographed for leaf area determination, then oven dried and weighed for SLA. V_o/V_c and the proportion of photosynthesis inhibited by ambient oxygen was determined with a 6400-40 leaf chamber fluorometer attachment. Leaves were given 15–20 min to adjust to the following chamber conditions: CO_2 was supplied at the growth room CO_2 level, light was supplied at 550 µmol PAR m^{-2} s^{-1}, leaf temperature was 21 °C, flow rate was 300 µmol s^{-1} and sample RH was maintained near 65%. V_o/V_c was calculated as per Bellasio *et al.* (2014) and the proportion of net photosynthesis inhibited by ambient oxygen was calculated as: $100\times[1-(A_{20}/A_2)]$, where A_{20}=net photosynthesis at ambient O_2 and A_2=net photosynthesis at 2% oxygen.

Harvest

Plants were destructively harvested after 29–30 d regrowth and divided into 'leaf' (5 cm above the pot surface), 'sheath' (0–5 cm from the pot surface), and roots. Leaf subsamples were taken from plants treated with 3, 5, 7.5, and 10 mM N, snap-frozen in liquid N, stored at –80 °C, then freeze-dried, ground to a powder, and analysed. Leaf subsamples were taken towards the end of the photoperiod (between 14.00 h and 22.00 h) in order to maximize differences in genotype leaf WSC levels during the natural diurnal cycle. The remaining leaf material was oven-dried at 65 °C for 4–6 d then weighed. Roots were cleaned and oven dried at 65 °C for 4–6 d before weighing. The fraction of biomass allocated to leaves (LMF) was calculated by dividing leaf DW by total plant DW. RGR was calculated from differences in paired plant DW, determined after defoliation (Supplementary Fig. S1) and after the regrowth phase. A non-biased plant pairing method (Poorter, 1989*a*) was used, based on end of establishment leaf DW. RGR calculation eliminated possible confounding differences in absolute DW data arising from clonal propagation (Beechey-Gradwell *et al.*, 2018).

Lipid and carbohydrate analyses

The freeze-dried and ground leaves were analysed for FAs and WSCs. FAs were extracted from 10–15 mg of ground sample and methylated in hot methanolic HCl, then quantified against a C15:0 internal standard by GC-MS (Browse *et al.*, 1986). Total FA concentration was calculated as the sum of palmitic acid (16:0), palmitoleic acid (16:1), stearic acid (18:0), oleic acid (18:1), linoleic acid (18:2), and linolenic acid (18:3) concentration in the leaves. The protocol for TAG extraction was as described in Winichayakul *et al.* (2013) without modification. For WSCs, a 25 mg sample of ground material was mixed twice with 1 ml of 80% ethanol and incubated at 65 °C for 30 min. After each extraction, the homogenate was centrifuged at 13 000 rpm for 10 min and the supernatant containing low molecular weight (LMW) WSCs was removed. High molecular weight (HMW) WSCs were extracted by twice mixing the remaining insoluble residue with 1 ml of water, then incubating, centrifuging, and removing the supernatant. Aliquots of these extracts were diluted then reacted with 1.25% anthrone in a mixture of H_2SO_4 and ethanol (3:5 v/v). The blue-green colour produced from the reaction was read at 620 nm. LMW and HMW WSCs were calibrated against a series of sucrose and inulin standards, respectively.

Statistical analysis

A complete randomized study design was used to investigate the relationship between genotype, CO_2, N form, and N concentration on various growth, morphology, and gas exchange parameters, leaf FAs, and leaf WSCs. Two- or three-way ANOVA was used to compare the gas exchange, leaf structure, and fluorescence data (collected at a single N concentration). For growth parameters, N concentration was treated as a continuous variable. For leaf FAs and leaf WSCs, N concentration was treated as a factor. A forward stepwise procedure was used for selecting variables. Variables and interaction terms with a P-value of <0.05 were retained in the final model. Due to residual heteroskedasticity, total plant DW data were log-transformed before modelling. Treatment means were compared and post-hoc multiple comparison P-values were adjusted using the Benjamini–Hochberg (BH) method. Raw means and SE values are presented in the tables and figures, while P-values in the tables and text were obtained from the final statistical models. All statistical analyses were performed in R (version 3.4.3, R Foundation).

Results

Leaf fatty acid and protein expression

In an initial screen of the transgenic material, there was no significant difference between WT and VC leaf FAs, while the cys-OLE/DGAT lines contained 23–100% more leaf FAs (4.3–7.0% DW) than the WT (3.5% DW) (Fig. 1A). Leaf FA concentration correlated closely with the expression of cys-OLE (Fig. 1B), but not DGAT (Fig. 1C). Leaf TAG accumulated to 2.5% DW in the highest expressing cys-OLE/DGAT line, compared with 0.18% DW in the WT (Supplementary Table S2). Root FAs were 10% and ~50% higher in the VC and cys-OLE/DGAT lines, respectively, than in the WT (Supplementary Table S2). Upon arranging the cys-OLE/DGAT lines according to leaf FA concentration, a possible leaf expansion and/or regrowth advantage relative to the WT and VC was visually observed in the cys-OLE/DGAT lines with a leaf FA concentration of ~5–6% DW (including 3501 and 6205), but not in the highest expressing cys-OLE/DGAT line (3807) with a leaf FA concentration of ~7% DW (Supplementary Fig. S2).

Leaf C storage

In the main experiment described in this study, the high expressing cys-OLE/DGAT genotype '6205' (HL) had a substantially higher (67–96%) leaf FA concentration than the WT under two CO_2 levels and 1–10 mM N supply (genotype effect $P<0.001$) (Fig. 2A). For both WT and HL, the maximum total leaf FA concentration was 24–32% lower in the main experiment than in the initial screen of glasshouse-regrown material (Fig. 1A). For both the WT and HL, total leaf FA concentration decreased slightly at e[CO_2] and increased with increasing N supply up until 5–10 mM, before stabilizing (Fig. 2A). HL leaf WSC concentration was substantially lower than in the WT under both a[CO_2] and e[CO_2] (genotype effect $P<0.001$) (Fig. 2B, C), especially in the HMW fraction (primarily fructans) which was 3- to 5-fold lower for HL than WT leaves at 7.5–10 mM N supply (Fig. 2C). Leaf WSC was higher at e[CO_2] (Fig. 2B, C), and tended to decrease with increasing NO_3^- supply (N form×N concentration interaction, $P<0.01$) (data not shown). Since FAs contain more energy and C than carbohydrates, the total C stored as leaf FA and WSC was calculated for each genotype. The overall differences in WT and HL leaf C storage (Fig. 2E) were such that the total concentration of C stored as leaf FA and WSC combined was substantially less in HL than in the WT (Fig. 2D).

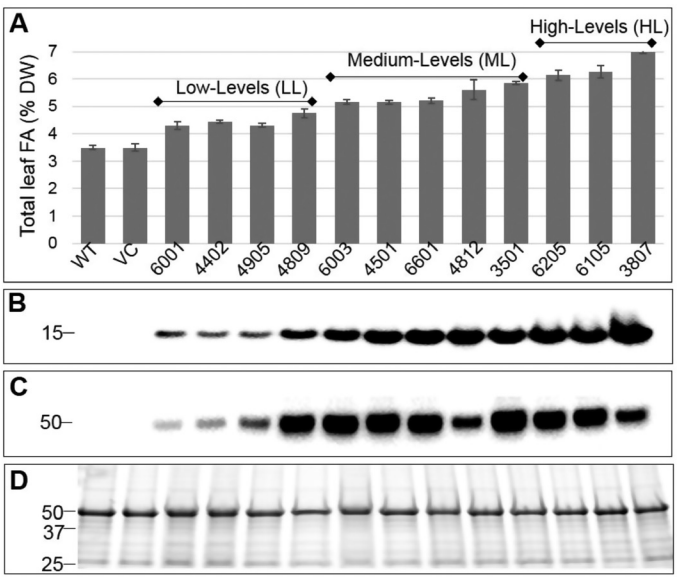

Fig. 1. Total leaf FA and relative recombinant protein (cys-OLE and DGAT) content of 12 independent ryegrass transformants. Samples were taken from leaf regrowth 3 weeks after propagation and cutting. (A) Total leaf FA as a percentage of DW; bars represent averages (n=6–8) ±SE. (B) Relative recombinant cys-OLE content. (C) Relative recombinant DGAT content. (D) Bio-Rad stain-free SDS–PAGE image showing equal loading of protein in each gel. The positions of the protein molecular weight markers are indicated in kDa. WT wild type; VC, vector control.

Growth

After 28–29 d regrowth under the different [CO_2] and N treatments, total plant dry biomass (DW) increased by 7- to 23-fold. For both the WT and HL, DW was greater under e[CO_2] than a[CO_2] and increased with N supply up until 4–10 mM (N concentration effect $P<0.001$), then stabilized or decreased thereafter (quadratic N concentration effect $P<0.001$). The DW of (defoliated) plants at the end of the establishment phase was 18% greater for WT than for HL plants ($P<0.01$ Student's t-test) (Supplementary Fig. S1). By the final harvest, however, HL DW was greater than that of the WT at high N supply, and similar at low N supply (genotype×N concentration interaction, $P<0.05$) (Fig. 3A, B). The RGR between post-establishment defoliation and the final harvest was also greater for HL than the WT, and at most levels of N supply (genotype effect, $P<0.001$) (Fig. 3C, D). DW was slightly greater under high NO_3^- supply compared with high NH_4^+ supply (N form×concentration interaction, $P<0.05$) (data not shown), but the increase in DW that occurred at e[CO_2] relative to a[CO_2] was similar with NO_3^- and NH_4^+ (i.e. no CO_2×N form interaction occurred) (data not shown).

Morphology

The fraction of biomass allocated to leaves (LMF) increased with increasing N supply up until 5–7.5 mM, then stabilized thereafter (quadratic N concentration effect, $P<0.001$) (Fig. 3E, F). LMF was substantially lower for HL at low N supply, but this difference became progressively smaller as N supply increased, such that at 7.5 mM N supply, HL had only a slightly lower LMF than the WT (10% when averaged across [CO_2] levels and N forms) (quadratic N concentration×genotype interaction, $P<0.001$) (Fig. 3E, F). HL had a correspondingly larger fraction of biomass allocated to roots than the WT and a similar fraction of biomass allocated to sheath (data not shown). At 7.5 mM N supply, HL had a substantially higher SLA than the WT (52% when averaged across [CO_2] levels and N forms) (genotype effect, $P<0.001$) (Table 1). For both the WT and HL, SLA was lower at e[CO_2] than a[CO_2] and higher under NO_3^- than NH_4^+ supply (Table 1). HL plants had a higher projected total leaf area to total plant DW ratio than the WT (35% when averaged across [CO_2] levels and N forms).

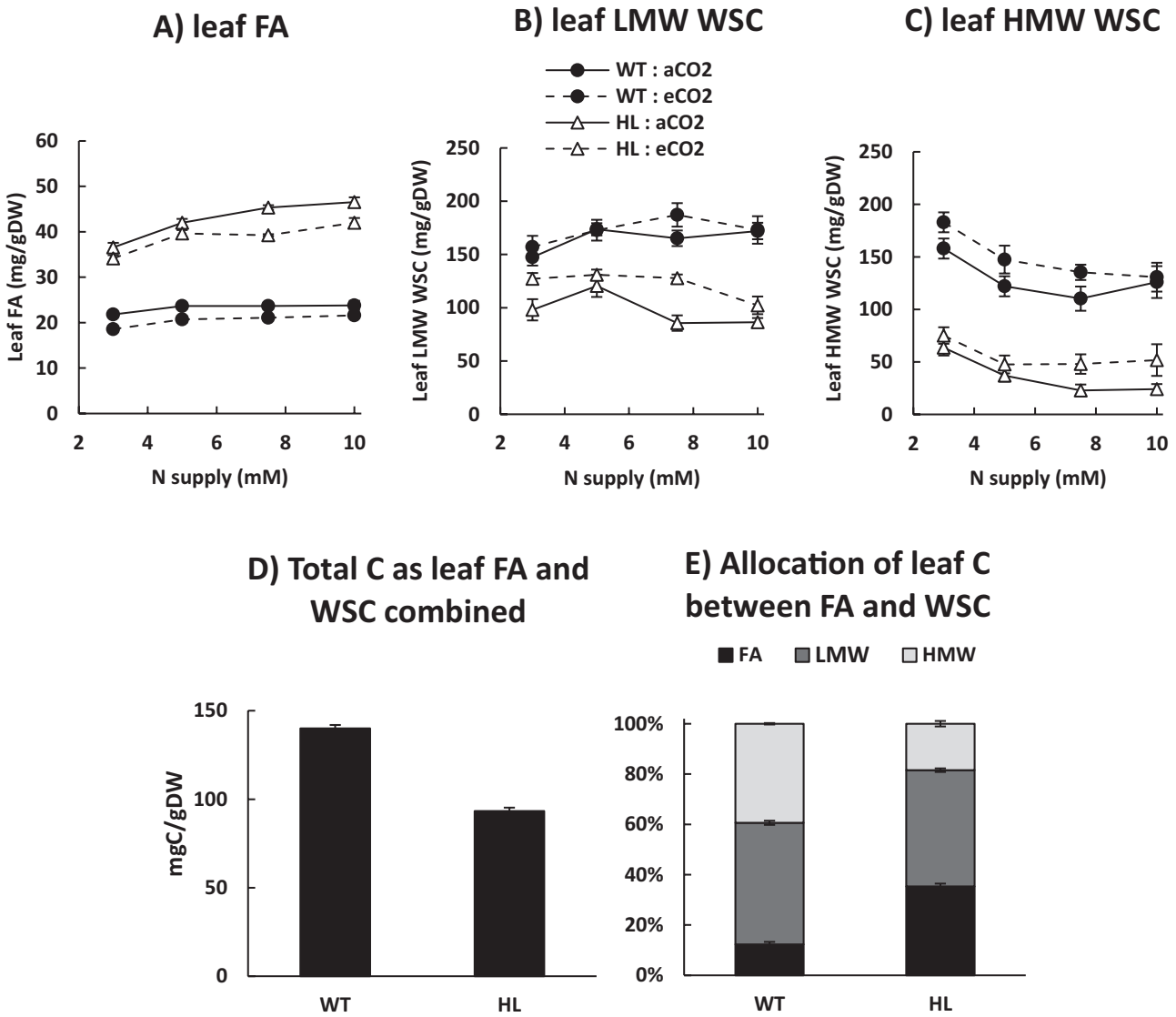

Fig. 2. Leaf C storage of a clonal cys-OLE/DGAT ryegrass transformant (HL, open triangles) and a wild-type control (WT, filled circles) genotype. (A) Leaf fatty acids (FAs), (B) LMW (low molecular weight) leaf water-soluble carbohydrates (WSCs), (C) HMW (high molecular weight) leaf WSCs, (D) total C allocated to leaf FA and WSC combined, (E) the proportions of leaf C as FA and WSC relative to one another (where 100%=total leaf C allocated to these potential storage pools). Plants were regrown for 28–29 d after defoliation at 1–10 mM N supply at either ambient (400 ppm) or elevated CO_2 (760 ppm). In (A–C). data points represent raw averages for plants regrown under NO_3^- and NH_4^+ (n=10) ±SE. In (D) and (E), bars represent an average over all N and CO_2 treatments (n=80) ±SE. aCO_2, ambient CO_2, eCO_2,elevated CO_2.

Gas exchange

HL displayed a higher A_{sat} than the WT at a[CO_2] (genotype effect, P<0.001) (Table 1). Similar results were also obtained when A was measured at growth room irradiance (A_{amb}) (data not shown). For both the WT and HL, A_{sat} increased and g_s decreased at e[CO_2] (CO_2 effect, P<0.001); however, the increase in A_{sat} at e[CO_2] compared with a[CO_2] was greater for HL than for the WT (genotype×CO_2 interaction, P<0.01) (Table 1). Relative to NO_3^- supply, NH_4^+ increased HL A_{sat} (by 9%) and decreased WT A_{sat} (by 29%) (genotype×N form interaction, P<0.001). Within [CO_2] treatments, light-saturated g_s and A_{area} correlated well (R^2=0.79 under a[CO_2] and 0.74 under e[CO_2], respectively) (Supplementary Fig. S3), and the ratio of leaf intracellular CO_2 to ambient CO_2 concentration (C_i/C_a) did not differ between the WT and HL, regardless of [CO_2] level or N form (Table 1).

A/C_i analysis, carried out for plants supplied with NO_3^- only, showed that HL had a substantially higher A_{sat} at low (Rubisco-limited) C_i (68–83% at 69–72 ppm C_i) compared with the WT. This difference became smaller at high (ribulose bisphosphate regeneration-limited) C_i (10–12% at 1023–1099 ppm C_i) (Fig. 4). The modelled maximum velocity of Rubisco carboxylation ($V_{c,max}$) decreased at e[CO_2] (CO_2 effect, P<0.01), especially for the WT (Supplementary Table S3). HL had a greater Φ PSII than the WT (genotype effect, P<0.001) and a lower V_o/V_c and percentage inhibition of A_{amb} at 20% O_2 than the WT (genotype effect, P<0.001) (Table 2). V_o/V_c and the inhibition of A_{amb} at 20% O_2 decreased at e[CO_2] (CO_2 effect, P<0.001), and V_o/V_c also decreased with NH_4^+ compared with NO_3^- supply (N form effect, P<0.05) (Table 2).

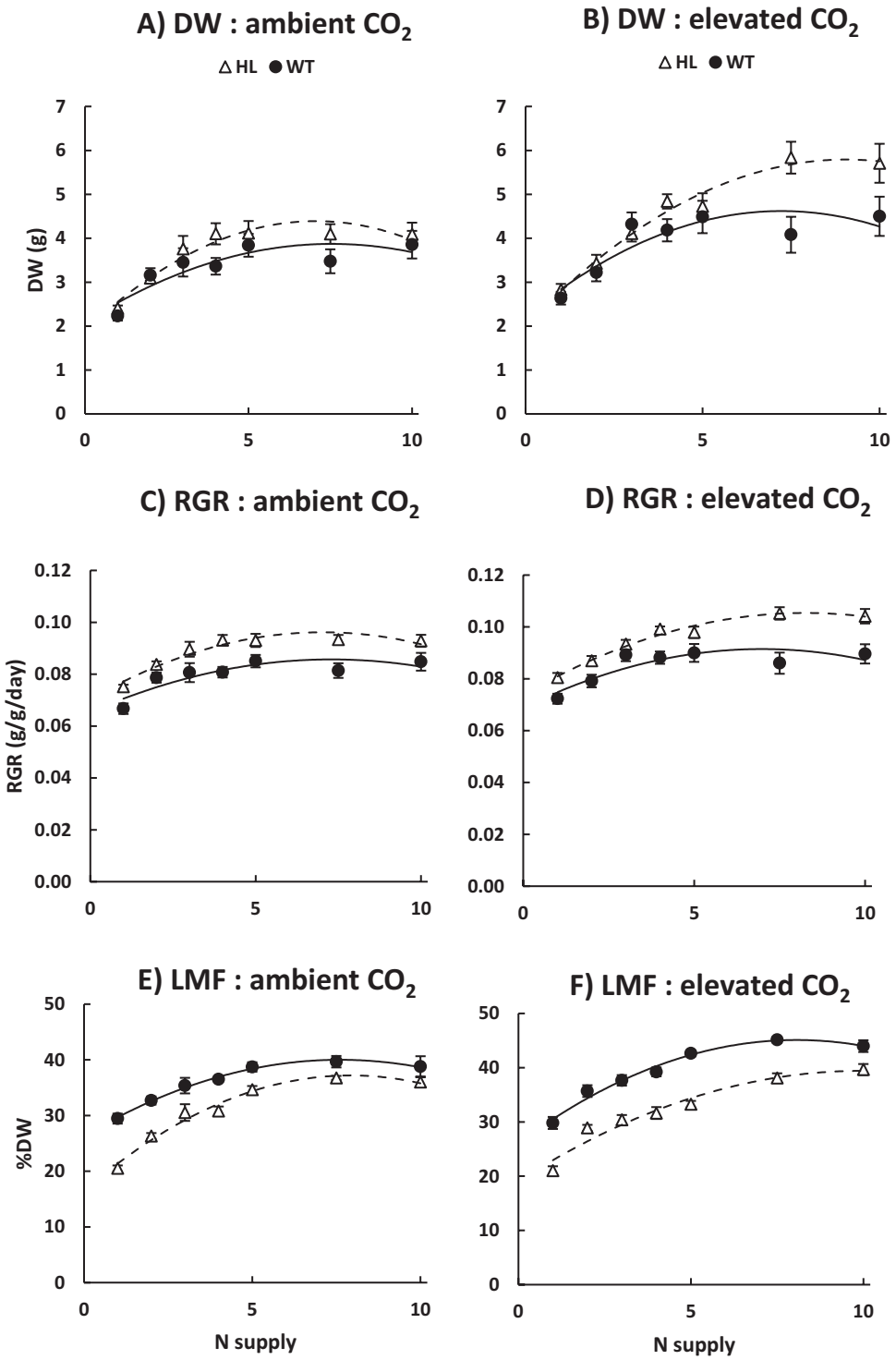

Fig. 3. Growth parameters of a clonal cys-OLE/DGAT ryegrass transformant (HL, open triangles) and a wild-type control (WT, filled circles) genotype. (A and B) Total plant DW, (C and D) relative growth rate (RGR), (E and F) the proportion of total plant DW allocated to leaves (LMF). Plants were regrown for 28–29 d after defoliation at 1–10 mM N supply at either ambient (400 ppm) or elevated CO_2 (760 ppm). Data points represent raw averages for plants regrown under NO_3^- and NH_4^+ (n=10) ±SE

Discussion

Cys-OLE/DGAT expression confers a lipid carbon sink in leaves and a growth advantage

Manipulation of many genes and gene combinations has been used to increase non-seed lipid content (see Vanhercke *et al.*, 2019, and references therein). However, the cys-OLE/DGAT technology remains the only reported case that increases plant biomass. Perennial ryegrass leaves expressing cys-OLE/DGAT contained up to double the leaf FA concentration (4.3–7% DW) and up to 14-fold more leaf TAG (2.5% DW) than a WT control. Leaf FA and TAG concentration correlated positively with the expression of cys-OLE (Fig. 1), confirming the efficacy of a 'package and protect' strategy (Vanhercke

Table 1. Specific leaf area (SLA), light-saturated photosynthetic rate per unit leaf area (A_{sat}), stomatal conductance (g_s), photosynthesis per unit of leaf mass (A_{mass}), and ratio of leaf intracellular CO_2 to ambient CO_2 concentration (C_i/C_a) of a clonal cys-OLE/DGAT ryegrass transformant (HL) and a wild-type control (WT) genotype

CO_2	N form	Genotype	SLA (cm^2 g DW^{-1})	A_{sat} (µmol CO_2 m^{-2} s^{-1})	g_s (CO_2 m^{-2} s^{-1})	A_{mass} (µmol CO_2 g DW^{-1} s^{-1})	C_i/C_a
Ambient	NO_3^-	WT	211±9 c	19.1±0.9 d	0.32±0.03 b	0.41±0.03 d	0.71±0.01 ab
		HL	290±8 a	23.3±0.2 c	0.40±0.01 a	0.68±0.02 b	0.71±0.01 ab
	NH_4^+	WT	155±3 de	15.6±0.6 e	0.22±0.01 d	0.24±0.01 e	0.67±0.01 bc
		HL	244±9 b	24.8±1.2 c	0.36±0.02 ab	0.60±0.02 c	0.66±0.01 c
Elevated	NO_3^-	WT	174±11 d	25.3±0.9 c	0.23±0.02 d	0.44±0.04 d	0.72±0.02 a
		HL	277±9 a	30.8±0.6 b	0.30±0.02 bc	0.85±0.01 a	0.73±0.02 a
	NH_4^+	WT	150±7 e	18.8±0.9 d	0.13±0.01 e	0.29±0.03 e	0.67±0.02 bc
		HL	231±3 bc	34.6±1.1 a	0.25±0.02 cd	0.80±0.03 a	0.66±0.02 c
		G	***	***	***	***	–
		N	***	–	***	***	***
		CO_2	**	***	***	***	–
	ANOVA	GxN	–	***	–	**	–
		$GxCO_2$	–	**	–	***	–
		$NxCO_2$	–	–	–	–	–
		$GxNxCO_2$	–	*	–	–	–

Plants were regrown at 7.5 mM N supply at either ambient (400 ppm) or elevated CO_2 (760 ppm)
Data points represent the raw averages of plants regrown under NO_3^- or NH_4^+ (n=5) ±SE. G, genotype effect, N, N form effect, CO_2, CO_2 effect significant in a three-way ANOVA. *P<0.05; **P<0.01; ***P<0.001. Different letters indicate statistically significant differences in predicted means obtained from three-way ANOVA, with P-values adjusted according to the BH method.

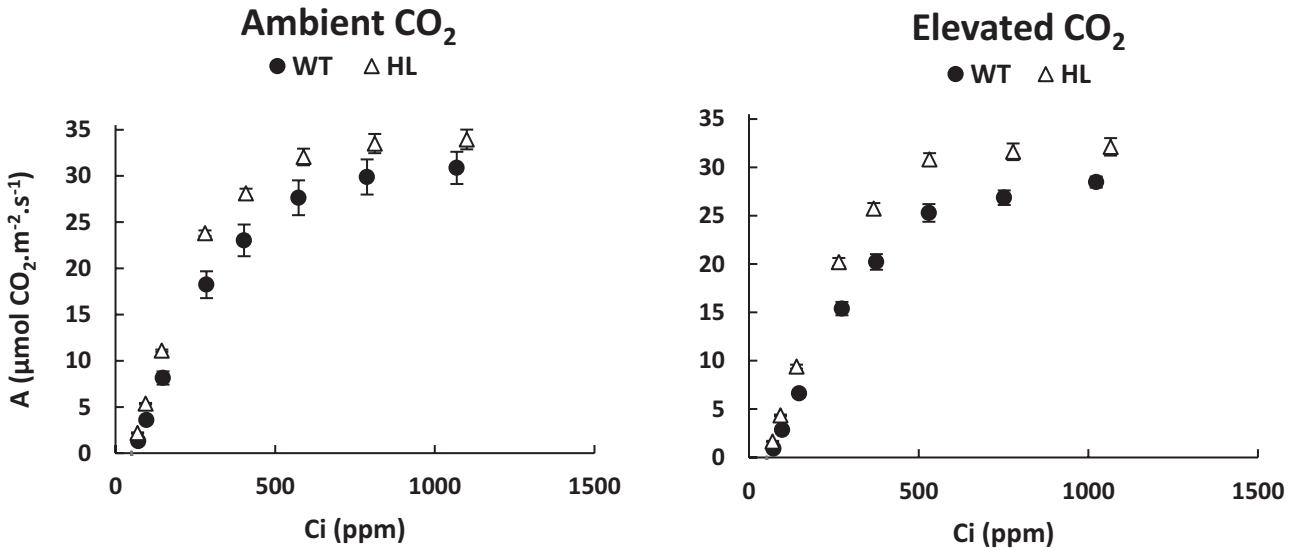

Fig. 4. Response of net photosynthesis per unit leaf area (A) to intracellular CO_2 concentration (C_i) of a clonal cys-OLE/DGAT ryegrass transformant (HL, open triangles) and a wild-type control (WT, filled circles) genotype. Plants were regrown at 5 mM NO_3^- supply under ambient (400 ppm) and at 7.5mM NO_3^- supply under elevated CO_2 (760 ppm). Data points represent the raw averages (n=5) ±SE.

et al., 2014) for accumulating lipids *in planta* (Winichayakul *et al.*, 2008, 2013). In the selected high expressing cys-OLE/DGAT line '6205' (HL), an increase in leaf FA concentration of 67–96% coincided with a decrease in total leaf WSC concentration of 68–170% compared with a WT control across the N and [CO_2] treatments (Fig. 2). For both the WT and HL, total plant DW was greater under e[CO_2] than a[CO_2] and increased with N supply up until 4–10 mM then stabilized or decreased thereafter. These growth responses to N availability and e[CO_2] are similar to those reported previously for other crop plants (Andrews *et al.*, 2019). Total plant DW at harvest was 7–24% greater for HL than the WT at medium to high N supply (4–10 mM), and similar for the two lines at low N supply (Fig. 3A, B). We used T_0 transgenics in this experiment, which required clonal propagation to generate replicates. Since changes in plant DW are proportional to the biomass present at the beginning of a period (Causton and Venus, 1981), an RGR measurement was used to account for possible differences in plant size at the beginning of the growth measurement phase (i.e. the regrowth) (Supplementary Fig. S1). The RGR between post-establishment defoliation and the final harvest was also greater for HL than the WT at most levels of N supply

Table 2. Quantum efficiency of PSII (Φ PSII), ratio of Rubisco oxygenation/carboxylation (V_o/V_c), and the proportion of photosynthesis inhibited by ambient oxygen of a clonal cys-OLE/DGAT ryegrass transformant (HL) and a wild-type control (WT) genotype

CO_2	N form	Genotype	Φ PSII	V_o/V_c	% inhibition of A_{amb} at 20% O_2
Ambient	NO_3^-	WT	0.42±0.02	0.35±0.02	34±1
		HL	0.54±0.01	0.29±0.01	29±1
	NH_4^+	WT	0.40±0.02	0.41±0.02	37±2
		HL	0.54±0.01	0.31±0.03	30±2
Elevated	NO_3^-	WT	0.40±0.01	0.18±0.01	15±2
		HL	0.55±0.01	0.13±0.01	8±2
	NH_4^+	WT	ND	ND	ND
		HL	ND	ND	ND
		G	***	***	***
		N	–	*	–
	ANOVA	CO_2	–	***	***
		GxN	–	–	–
		GxCO_2	–	–	

Plants were regrown at 5 mM N supply at either ambient (400 ppm) or elevated CO_2 (760 ppm).
Data points represent the raw averages of plants regrown under NO_3^- or NH_4^+ (n=5) ±SE. A_{amb}, photosynthesis at growth room irradiance; G, genotype effect; N, N form effect; CO_2, CO_2 effect significant in a three-way ANOVA. *P<0.05; **P<0.01; ***P<0.001. ND, not determined.

(Fig. 3C, D). Our finding that cys-OLE/DGAT expression can enhance plant growth is consistent with observations in Arabidopsis (Winichayakul *et al.*, 2013).

Reasons for the growth advantage with cys-OLE/DGAT expression in leaves: increased SLA and A_{area}

RGR was greater for HL than the WT at most N levels under a[CO_2] and e[CO_2], indicating that net photosynthesis per plant was greater for HL than the WT under most treatments. However, LMF was lower for HL than the WT under most treatments (Fig. 3E, F). Also, leaf DW was lower for HL than the WT under all but the highest levels of N supply (7.5–10 mM). Therefore, greater photosynthesis per HL plant was not explained by greater allocation of DW to leaves, which was, on the other hand, a factor linked to increased growth with increased N supply for both HL and the WT. An increase in both SLA and A_{area} could account for the increase in the HL RGR, consistent with data from a preliminary experiment (Supplementary Table S4). SLA, multiplied by the proportion of DW allocated to leaves (LMF), determines the total leaf area per unit of plant DW, which strongly dictates light interception and growth rate (Poorter, 1989*b*). HL had a slightly lower LMF than the WT at 7.5 mM N supply, but a much higher SLA (Table 1), and therefore a higher projected total leaf area to total plant DW ratio than the WT. A medium to high N supply (4–10 mM) maximized the RGR difference between the HL and WT (Fig. 3C, D). Two morphological features could have contributed to this altered growth response to N in cys-OLE/DGAT ryegrass. First, HL allocated substantially less biomass to leaves at low N supply, but HL LMF increased more steeply as N supply increased. Secondly, since a high SLA generally increases photosynthetic N use efficiency (Poorter, 1989*b*), the C gain per incremental increase in leaf N may be higher for a cys-OLE/DGAT leaf.

Although approximately half of the HL SLA advantage could be directly accounted for by the lower combined FA and WSC concentration in the HL leaves, it was still highly significant when SLA was calculated on an FA- and WSC-free (i.e. structural) basis. Across five cys-OLE/DGAT ryegrass lines, SLA was positively correlated with leaf FA concentration (Luke Cooney, unpublished data), indicating a possible causal relationship between leaf lipid accumulation and the increase in SLA (see also Supplementary Table S4). The mechanisms governing SLA plasticity have not been studied in detail, but SLA generally increases under conditions of low C availability/low carbohydrate accumulation, such as low light (Poorter *et al.*, 2009), or, specifically, when the sink:source ratio increases in perennial ryegrass due to frequent defoliation (Lee *et al.*, 2010). In both of these cases, increased SLA is associated with an allocation adjustment towards an increased LMF, although a regulatory link between leaf carbohydrate levels and SLA or LMF (or shoot to root ratio) has not been established (Andrews *et al.*, 2006; Poorter *et al.*, 2009). Here, the increase in HL SLA was associated with low leaf carbohydrates, but unexpectedly also coincided with a decreased LMF. The trade-off between FA and WSC accumulation in HL leaves suggests that cys-OLE-encapsulated lipid droplets behave as an additional energy-consuming C sink in leaves, with sufficient strength to induce a large shift in the instantaneous leaf energy balance, and perhaps even penalize leaf growth under some conditions. However, the biomass of the HL sheath and root system was greater than for the WT, implying that there was no long-term penalty to the export of C from leaves to sink organs. Further work will explore DW and C partitioning and diurnal variation in WSC, FA, and gross energy within and between different cys-OLE/DGAT ryegrass organs.

The increase in HL photosynthesis at 7.5 mM N supply was coupled to an increase in stomatal conductance (g_s) (Supplementary Fig. S3). Across diverse growth conditions, g_s coordinates closely with the CO_2 requirement of the mesophyll such that the C_i/C_a ratio remains constant (Wong *et al.*, 1979). In this experiment, C_i/C_a did not differ between the WT and HL, implying that the HL mesophyll was a stronger sink for CO_2. A/C_i analysis showed that an increase in HL A at low C_i occurred which was independent of g_s (Fig. 4).

Common explanations for a steeper A/C_i curve at low (Rubisco-limited) C_i include increased Rubisco carboxylation efficiency and/or content per leaf area, or increased mesophyll conductance to CO_2 (g_m). We investigated the CO_2/O_2 ratio in the chloroplast in order to assess possible changes in Rubisco carboxylation efficiency associated with a possible 'CO_2 recycling' phenomenon occurring in cys-OLE/DGAT leaves (Winichayakul *et al.*, 2013). Compared with a WT control, HL displayed a decrease in two measures of photorespiration (Table 2), which coincided with increased photosynthetic sensitivity to e[CO_2] (Table 1) and a higher CO_2 compensation point (Supplementary Table S1A). In contrast, decreased photosynthetic sensitivity to e[CO_2] and a lower CO_2 compensation point were observed in Arabidopsis plants engineered to have lower photorespiration and a greater CO_2/O_2 ratio in the chloroplast (Kebeish *et al.*, 2007). Thus, our gas exchange data did not support the hypothesis that CO_2 recycling makes an important contribution to the increase in cys-OLE/DGAT photosynthesis (Winichayakul *et al.*, 2013).

We did not quantify Rubisco or g_m in this study, but we contend that the large increase in HL SLA makes increased Rubisco per leaf area less likely than an increase in g_m to explain the steeper A/C_i response in HL leaves at low C_i. HL plants regrown at 5 mM NO_3^-, for example, had a 56% greater SLA than the WT, so an approximate doubling in leaf Rubisco concentration would have been required to deliver the 35–40% increase in HL A at a C_i of ~150 ppm. Greater g_m is an important mechanism by which leaves with an inherently high SLA achieve greater photosynthetic efficiency than low SLA leaves (Onoda *et al.*, 2017). Parameterization of the A/C_i curves (Sharkey *et al.*, 2007) gave a high estimate of g_m for HL (Supplementary Table S3), but such estimations of g_m are unreliable, and so further work will be needed here. Finally, since Φ PSII contributes to photosynthetic efficiency and is modulated by various stresses, we sought to show that the differences in Φ PSII and photosynthesis between the WT and HL (Table 2) were unrelated to photoinhibition 'stress' in the WT, by measuring these parameters alongside the maximum quantum efficiency of PSII (F_v/F_m). The increase in HL photosynthesis and Φ PSII coincided with a very small (~1%) increase in F_v/F_m compared with the WT (Supplementary Table S1B). This suggested that photoinhibition 'stress' in the WT could not explain the increase in cys-OLE/DGAT photosynthesis.

Why would leaf cys-OLE/DGAT expression make photosynthesis more responsive to e[CO_2] at high N supply?

Expression of cys-OLE/DGAT in ryegrass leaves enhanced the stimulation of light-saturated photosynthesis at e[CO_2] at 7.5 mM N supply (Table 1), consistent with results from a preliminary experiment (Supplementary Table S4). Parameterization of the A/C_i curves at a[CO_2] and e[CO_2] suggested that cys-OLE/DGAT expression also reduced the severity of photosynthetic down-regulation at e[CO_2] (Supplementary Table S3). Interestingly, the changes in mass-based photosynthesis (A_{area}×SLA=A_{mass}) at e[CO_2] were modulated by changes not only in A_{area} but also in SLA. Under NO_3^- supply, HL SLA did not significantly decrease at e[CO_2], while WT SLA did significantly decrease at e[CO_2] (Table 1). A_{mass} correlates better with growth than A_{area} in spaced pots (Poorter, 1989*b*) and typically changes less than A_{area} with changes in atmospheric [CO_2] due to compensatory changes in SLA (Poorter *et al.*, 2009; Temme *et al.*, 2017).

When the sink:source ratio decreases, carbohydrates generally accumulate in the leaves (Paul and Foyer, 2001). This was well illustrated in this study; increasing the CO_2 supply (increasing source activity) or decreasing NO_3^- supply (decreasing sink development) caused the leaf WSC concentration to increase (Fig. 2B, C). Due to the limited capacity of perennial ryegrass to produce new sinks, leaf carbohydrates can build up rapidly upon exposure to e[CO_2], leading to potentially severe photosynthetic acclimation (Fischer *et al.*, 1997). In free air CO_2 enrichment trials, however, perennial ryegrass sustained large increases in photosynthesis at e[CO_2] when practices that increased the canopy sink:source ratio, such as regular defoliation and N fertilizer application, were employed (Ainsworth *et al.*, 2003; Guo *et al.*, 2006). In this study, HL leaf WSC concentration increased at e[CO_2], but not beyond the levels in WT leaves regrown at a[CO_2]. We speculate that the diversion of carbohydrate into a lipid C sink could mitigate signals to down-regulate photosynthesis in a WT ryegrass leaf at e[CO_2], and thus cys-OLE/DGAT expression could allow a greater magnitude of photosynthetic stimulation at e[CO_2].

Unexpectedly, we found that NH_4^+ supply (compared with NO_3^-) increased A_{sat} for HL whereas the reverse effect occurred for the WT control (Table 1). We observed minor growth toxicity symptoms in the WT at high NH_4^+ supply (7.5–10 mM), suggesting that this may have been a consequence of different capacities for NH_4^+ assimilation and detoxification (possibly due to a larger root system for HL). Otherwise, the form of N had general effects on processes relating to photosynthesis and growth which were independent of genotype or [CO_2] level. Plants supplied with NH_4^+ had a lower SLA, A_{mass}, g_s, and C_i/C_a than plants supplied with NO_3^- (Table 1). The maximum DW achieved was also lower under NH_4^+ supply than NO_3^-. While not significant, we observed a slightly greater magnitude of DW stimulation at e[CO_2] under NO_3^- supply (32% and 44% for the WT and HL, respectively) compared with NH_4^+ supply (17% and 24% for the WT and HL, respectively). Therefore, our perennial ryegrass regrowth data provide little evidence to support the claim that stimulation of growth by e[CO_2] is inhibited under NO_3^- supply in C_3 plants (Bloom, 2015). This finding agrees with recent results for wheat published by Andrews *et al.* (2019).

Could storing lipids in leaves improve yield?

It has been speculated previously that introducing a new sink in the form of TAG in leaves might influence photosynthesis (Xu and Shanklin, 2016; Vanhercke *et al.*, 2017, 2019), but few measurements related to photosynthesis or C assimilation have been reported for high TAG plants. Transgenic rice expressing the glycerol-3-phosphate dehydrogenase enzyme with high plastid lipids exhibited enhanced CO_2 assimilation (Singh *et al.*, 2016). Up-regulation of photosynthetic genes occurred in high TAG/low starch tobacco overexpressing WR1,

DGAT1, and OLE1 (Vanhercke *et al*., 2017), but broadly the opposite changes in gene expression occurred in tobacco leaves expressing WR1 alone, which coincided with decreased photosynthetic capacity (Grimberg *et al*., 2015). Changes in several photosynthetic parameters were absent in Arabidopsis mutants with various disruptions in starch synthesis and lipid metabolism, even though these mutations generated wide variation in leaf soluble sugar levels (Yu *et al*., 2018).

So why do many successful efforts to increase leaf TAG not increase photosynthesis and/or growth? Given the substantial energetic costs of FA synthesis, should maintaining even the same biomass as untransformed plants require that high TAG plants undergo changes delivering greater C assimilation? In many cases, manipulations of lipid metabolism result in growth penalties due to pleiotropic effects, or when TAG accumulates to very high levels, because competition for C inhibits normal development (Vanhercke *et al*., 2019). Indeed, cys-OLE/DGAT ryegrass lines with a leaf FA concentration above ~6.5% DW incur a growth penalty relative to controls (Beechey-Gradwell *et al*., 2018). Here it should be emphasized that the economic value of higher non-seed TAG could easily compensate for possible biomass penalties (Vanhercke *et al*., 2019). As well as the importance of optimizing lipid levels, we contend that the expression pattern is critical here. Green tissue-specific FA/TAG accumulation will enhance the probability of a positive growth effect by minimizing excessive competition for C by heterotrophic tissues (Winichayakul *et al*., 2013). We further speculate that lipid protection may be important, and, in this regard, the mechanism by which we propose that cys-OLE prevents lipid droplet breakdown may be relatively unique. We reported that cys-OLE conferred enhanced stability to lipid droplets in vegetative tissues, and *in vitro* in the presence of cysteine protease, whereas protection was not achieved with a native oleosin (Winichayakul *et al*., 2013). If futile cycles of TAG biosynthesis and catabolism followed by either FA recycling in the endoplasmic reticulum or β-oxidation impose a significant energetic penalty, then avoiding growth penalties may not be possible without TAG protection. Inhibiting lipid catabolic pathways (by, for example, silencing the activity of the TAG lipases) might be effective for this purpose (Kelly *et al*., 2013; Vanhercke *et al*., 2017) if normal processes are not disrupted. In plants with high concentrations of unprotected TAG and high rates of FA turnover, the fate of CO_2 released during the pyruvate to acetyl-CoA conversion may be important (Vanhercke *et al*., 2017) and confining CO_2 release to chloroplasts via green tissue-specific FA synthesis/TAG accumulation seems sensible (Schwender *et al*., 2004).

To maintain energy homeostasis and survive, it is critically important that plants can sense their carbohydrate status and respond by adjusting their physiological state appropriately (Smith and Stitt, 2007; Lee *et al*., 2010). For example, rates of starch synthesis and degradation are tightly regulated during the day to ensure a sufficient supply of C during the night, when CO_2 fixation is unavailable (Smith and Stitt, 2007). Plants with impaired starch synthesis have higher FA synthesis and turnover at night, suggesting that FAs become important respiratory substrates for normal growth in starchless mutants (Yu *et al*., 2018). Given their distinct natural functions in cells, lipid accumulation and remobilization may not be subject to the same fine-tuned regulation as carbohydrates, and inevitable losses of energy and C may occur when lipids function as an energy store (Yu *et al*., 2018). However, being the site of photosynthesis, well-illuminated leaves have an abundant local supply of energy and reductant. Our results show that under favourable growing conditions, the manipulation of lipid biosynthesis and storage can drive greater C assimilation. Further work will be needed to identify the optimal levels and expression patterns of FA/TAG accumulation, and how various strategies to package and protect accumulated TAG influence plant energy homeostasis and growth under other conditions.

Supplementary data

Fig. S1. End of establishment phase sheath and root DW of a defoliated clonal cys-OLE/DGAT ryegrass transformant and a wild-type control genotype.

Fig. S2. Visual comparison of 2 weeks of shoot regrowth of independent cys-OLE/DGAT lines with a wild-type and vector control genotype.

Fig. S3. Relationship between light-saturated photosynthetic rate per unit leaf area and stomatal conductance of a clonal cys-OLE/DGAT ryegrass transformant and a wild-type control genotype.

Table S1. CO_2 compensation point in the absence of dark respiration in the light, and F_v/F_m measured alongside the quantum efficiency of PSII and photosynthesis of a clonal cys-OLE/DGAT ryegrass transformant and a wild-type control genotype.

Table S2. Total leaf fatty acid, leaf triacylglycerol, and total root fatty acid of two independent clonal cys-OLE/DGAT ryegrass lines, a wild type, and a vector control genotype.

Table S3. Photosynthetic parameters derived from modelling the response of photosynthesis to intracellular CO_2 concentration of a clonal cys-OLE/DGAT ryegrass transformant and a wild-type control genotype.

Table S4. Preliminary analysis of specific leaf area, light-saturated photosynthetic rate per unit leaf area, leaf fatty acid and leaf water-soluble carbohydrate concentration of two independent clonal cys-OLE/DGAT ryegrass lines and a wild-type control genotype regrown at ambient and elevated CO_2.

Supplementary data are available at *JXB* online.

Acknowledgements

We would like to thank Kim Richardson and the transformation laboratory for generating the plant material, and Paul Newton and Greg Bryan for advice on the manuscript. This work was funded by Dairy NZ and MBIE contract C10X1603 and AgResearch SSIF.

References

Ainsworth EA, Davey P, Hymus G, Osborne C, Rogers A, Blum H, Nösberger J, Long S. 2003. Is stimulation of leaf photosynthesis by elevated carbon dioxide concentration maintained in the long term? A test with *Lolium perenne* grown for 10 years at two nitrogen fertilization levels under Free Air CO_2 Enrichment (FACE). Plant, Cell & Environment **26**, 705–714.

Ainsworth EA, Rogers A. 2007. The response of photosynthesis and stomatal conductance to rising [CO_2]: mechanisms and environmental interactions. Plant, Cell & Environment **30**, 258–270.

Ainsworth EA, Rogers A, Nelson R, Long SP. 2004. Testing the 'source–sink' hypothesis of down-regulation of photosynthesis in elevated [CO_2] in the field with single gene substitutions in *Glycine max*. Agricultural and Forest Meteorology **122**, 85–94.

Andrews M, Condron LM, Kemp PD, Topping JF, Lindsey K, Hodge S, Raven JA. 2019. Elevated CO_2 effects on nitrogen assimilation and growth of C_3 vascular plants are similar regardless of N-form assimilated. Journal of Experimental Botany **70**, 683–690.

Andrews M, Love B, Sprent J. 1989. The effects of different external nitrate concentrations on growth of *Phaseolus vulgaris* cv. Seafarer at chilling temperatures. Annals of Applied Biology, **114**, 195–204.

Andrews M, Raven J, Lea P. 2013. Do plants need nitrate? The mechanisms by which nitrogen form affects plants. Annals of Applied Biology **163**, 174–199.

Andrews M, Raven JA, Lea PJ, Sprent JI. 2006. A role for shoot protein in shoot–root dry matter allocation in higher plants. Annals of Botany **97**, 3–10.

Beechey-Gradwell ZD, Winichayakul S, Roberts NJ. 2018. High lipid perennial ryegrass growth under variable nitrogen, water and carbon dioxide supply. Journal of New Zealand Grasslands **80**, 219–224.

Bellasio C, Burgess SJ, Griffiths H, Hibberd JM. 2014. A high throughput gas exchange screen for determining rates of photorespiration or regulation of C_4 activity. Journal of Experimental Botany **65**, 3769–3779.

Bloom AJ. 2015. The increasing importance of distinguishing among plant nitrogen sources. Current Opinion in Plant Biology **25**, 10–16.

Browse J, McCourt PJ, Somerville CR. 1986. Fatty acid composition of leaf lipids determined after combined digestion and fatty acid methyl ester formation from fresh tissue. Analytical Biochemistry **152**, 141–145.

Causton DR, Venus JC. 1981. The biometry of plant growth. London: Edward Arnold.

Chapman D, Bryant J, McMillan W, Khaembah E. 2012. Economic values for evaluating pasture plant traits. Journal of New Zealand Grasslands **74**, 209–216.

Fischer B, Frehner M, Hebeisen T, Zanetti S, Stadelmann F, Lüscher A, Hartwig UA, Hendrey GR, Blum H, Nösberger J. 1997. Source–sink relations in *Lolium perenne* L. as reflected by carbohydrate concentrations in leaves and pseudo-stems during regrowth in a free air carbon dioxide enrichment (FACE) experiment. Plant, Cell & Environment **20**, 945–952.

Grimberg Å, Carlsson AS, Marttila S, Bhalerao R, Hofvander P. 2015. Transcriptional transitions in *Nicotiana benthamiana* leaves upon induction of oil synthesis by WRINKLED1 homologs from diverse species and tissues. BMC Plant Biology **15**, 192.

Guo J, Trotter CM, Newton PC. 2006. Initial observations of increased requirements for light-energy dissipation in ryegrass (*Lolium perenne*) when source/sink ratios become high at a naturally grazed free air CO_2 enrichment (FACE) site. Functional Plant Biology **33**, 1045–1053.

Guo S, Zhou Y, Shen Q, Zhang F. 2007. Effect of ammonium and nitrate nutrition on some physiological processes in higher plants—growth, photosynthesis, photorespiration, and water relations. Plant Biology **9**, 21–29.

Hofvander P, Ischebeck T, Turesson H, Kushwaha SK, Feussner I, Carlsson AS, Andersson M. 2016. Potato tuber expression of Arabidopsis WRINKLED1 increase triacylglycerol and membrane lipids while affecting central carbohydrate metabolism. Plant Biotechnology Journal **14**, 1883–1898.

Kebeish R, Niessen M, Thiruveedhi K, Bari R, Hirsch HJ, Rosenkranz R, Stäbler N, Schönfeld B, Kreuzaler F, Peterhänsel C. 2007. Chloroplastic photorespiratory bypass increases photosynthesis and biomass production in *Arabidopsis thaliana.* Nature Biotechnology **25**, 593–599.

Kelly AA, van Erp H, Quettier AL, Shaw E, Menard G, Kurup S, Eastmond PJ. 2013. The sugar-dependent1 lipase limits triacylglycerol accumulation in vegetative tissues of *Arabidopsis*. Plant Physiology **162**, 1282–1289.

Kingston-Smith A, Theodorou M. 2000. Tansley Review No. 118. Post-ingestion metabolism of fresh forage. New Phytologist **148**, 37–55.

Lee JM, Sathish P, Donaghy DJ, Roche JR. 2010. Plants modify biological processes to ensure survival following carbon depletion: a *Lolium perenne* model. PLoS One **5**, e12306.

Long SP, Zhu XG, Naidu SL, Ort DR. 2006. Can improvement in photosynthesis increase crop yields? Plant, Cell & Environment **29**, 315–330.

Napier JA, Haslam RP, Beaudoin F, Cahoon EB. 2014. Understanding and manipulating plant lipid composition: metabolic engineering leads the way. Current Opinion in Plant Biology **19**, 68–75.

Onoda Y, Wright IJ, Evans JR, Hikosaka K, Kitajima K, Niinemets Ü, Poorter H, Tosens T, Westoby M. 2017. Physiological and structural tradeoffs underlying the leaf economics spectrum. New Phytologist **214**, 1447–1463.

Paul MJ, Foyer CH. 2001. Sink regulation of photosynthesis. Journal of Experimental Botany **52**, 1383–1400.

Poorter H. 1989*a*. Plant growth analysis: towards a synthesis of the classical and the functional approach. Physiologia Plantarum **75**, 237–244.

Poorter H. 1989*b*. Interspecific variation in relative growth rate: on ecological causes and physiological consequences. In: Lambers H, ed. Causes and consequences of variation in growth rate and productivity of higher plants. The Hague, The Netherlands: SPB Academic Publishing Bv, 45–68.

Poorter H, Bühler J, van Dusschoten D, Climent J, Postma JA. 2012. Pot size matters: a meta-analysis of the effects of rooting volume on plant growth. Functional Plant Biology **39**, 839–850.

Poorter H, Niinemets U, Poorter L, Wright IJ, Villar R. 2009. Causes and consequences of variation in leaf mass per area (LMA): a meta-analysis. New Phytologist **182**, 565–588.

Schwender J, Goffman F, Ohlrogge JB, Shachar-Hill Y. 2004. Rubisco without the Calvin cycle improves the carbon efficiency of developing green seeds. Nature **432**, 779–782.

Sharkey TD. 2016. What gas exchange data can tell us about photosynthesis. Plant, Cell & Environment **39**, 1161–1163.

Sharkey TD, Bernacchi CJ, Farquhar GD, Singsaas EL. 2007. Fitting photosynthetic carbon dioxide response curves for C_3 leaves. Plant, Cell & Environment **30**, 1035–1040.

Singh V, Singh PK, Siddiqui A, Singh S, Banday ZZ, Nandi AK. 2016. Over-expression of *Arabidopsis thaliana* SFD1/GLY1, the gene encoding plastid localized glycerol-3-phosphate dehydrogenase, increases plastidic lipid content in transgenic rice plants. Journal of Plant Research **129**, 285–293.

Smith AM, Stitt M. 2007. Coordination of carbon supply and plant growth. Plant, Cell & Environment **30**, 1126–1149.

Temme AA, Liu JC, van Hal J, Cornwell WK, Cornelissen JH-H, Aerts R. 2017. Increases in CO_2 from past low to future high levels result in 'slower' strategies on the leaf economic spectrum. Perspectives in Plant Ecology, Evolution and Systematics **29**, 41–50.

Vanhercke T, Divi UK, El Tahchy A, *et al.* 2017. Step changes in leaf oil accumulation via iterative metabolic engineering. Metabolic Engineering **39**, 237–246.

Vanhercke T, Dyer JM, Mullen RT, Kilaru A, Rahman MM, Petrie JR, Green AG, Yurchenko O, Singh SP. 2019. Metabolic engineering for enhanced oil in biomass. Progress in Lipid Research **74**, 103–129.

Vanhercke T, Petrie JR, Singh SP. 2014. Energy densification in vegetative biomass through metabolic engineering. Biocatalysis and Agricultural Biotechnology **31**, 75–80.

White AC, Rogers A, Rees M, Osborne CP. 2016. How can we make plants grow faster? A source–sink perspective on growth rate. Journal of Experimental Botany **67**, 31–45.

Winichayakul S, Cookson R, Scott R, Zhou J, Zou X, Roldan M, Richardson K, Roberts NJ. 2008. Delivery of grasses with high levels of unsaturated, protected fatty acids. Journal of New Zealand Grasslands **70**, 211–216.

Winichayakul S, Scott RW, Roldan M, Hatier JH, Livingston S, Cookson R, Curran AC, Roberts NJ. 2013. In vivo packaging of triacylglycerols enhances Arabidopsis leaf biomass and energy density. Plant Physiology **162**, 626–639.

Wong S, Cowan I, Farquhar G. 1979. Stomatal conductance correlates with photosynthetic capacity. Nature **282**, 424.

Wu A, Hammer GL, Doherty A, von Caemmerer S, Farquhar GD. 2019. Quantifying impacts of enhancing photosynthesis on crop yield. Nature Plants **5**, 380–388.

Xu C, Shanklin J. 2016. Triacylglycerol metabolism, function, and accumulation in plant vegetative tissues. Annual Review of Plant Biology **67**, 179–206.

Yu L, Fan J, Yan C, Xu C. 2018. Starch deficiency enhances lipid biosynthesis and turnover in leaves. Plant Physiology **178**, 118–129.

Zale J, Jung JH, Kim JY, *et al.* 2016. Metabolic engineering of sugarcane to accumulate energy-dense triacylglycerols in vegetative biomass. Plant Biotechnology Journal **14**, 661–669.